



NIH PUBLIC ACCESS

Author Manuscript

*Lab Chip*. Author manuscript; available in PMC 2015 February 07.

Published in final edited form as:

*Lab Chip*. 2014 February 7; 14(3): 459–462. doi:10.1039/c3lc51160j.

## Oxygen Levels in Thermoplastic Microfluidic Devices during Cell Culture

**Christopher J. Ochs<sup>a,†</sup>, Junichi Kasuya<sup>b,†</sup>, Andrea Pavesi<sup>a,†</sup>, and Roger D. Kamm<sup>a,b,\*</sup>**<sup>a</sup> Singapore MIT Alliance for Research and Technology, BioSystems and Micromechanics, 1 CREATE Way, #04-13/14 Enterprise Wing, Singapore 138602<sup>b</sup> MechanoBiology Laboratory, Department of Biological Engineering, Massachusetts Institute of Technology, 77 Massachusetts Avenue, NE47-321, Cambridge, MA, 02139

### Abstract

We developed a computational model to predict oxygen levels in microfluidic plastic devices during cell culture. This model is based on experimental evaluation of oxygen levels. Conditions are determined that provide adequate oxygen supply to two cell types, hepatocytes and endothelial cells, either by diffusion through the plastic device, or by supplying a low flow rate of medium.

In recent years, microfluidic devices have been established as versatile platforms to mimic certain tissue microenvironments for the study of cellular behaviour and signalling. Due to its optical transparency, biocompatibility, gas permeability and ease of fabrication, polydimethylsiloxane (PDMS) is usually employed for lab-scale studies, but PDMS has disadvantageous characteristics in terms of adsorption of small hydrophobic species.<sup>1, 2</sup> Recent investigations into the oxygen distribution and manipulation inside devices demonstrate a growing interest in cell culture under hypoxic or anoxic conditions.<sup>3-6</sup> Here, thermoplastic devices made from cyclic olefin copolymer (COC), polystyrene (PS), or polypropylene (PP), poly(methacrylic acid) (PMMA) amongst others, offer an oxygen-impermeable alternative and are also easily mass-produced by means of hot embossing or injection-molding. Poly(methyl pentene) (PMP) is a new, promising material for normoxic microfluidic applications, because it combines excellent processability and biocompatibility with high oxygen permeability.<sup>7</sup> Numerous methods are reported to create leak- and burst-proof bonds between thermoplastic devices and films (homogeneous) or other materials (heterogeneous).<sup>8-12</sup> However, little is known about the oxygen levels inside thermoplastic microfluidic devices during cell culture and the possible impact on cell viability and behaviour. Studies propose that under long-term hypoxia/anoxia some cell types exhibit a reverse Pasteur effect, down-regulated oxygen consumption<sup>13</sup> and protein synthesis,<sup>14</sup> or altered gene expression.<sup>15</sup> It is therefore imperative to know the levels of oxygen prevailing in a given cell culture situation in order to make conclusions about cellular behaviour.<sup>16</sup>

© The Royal Society of Chemistry

<sup>\*</sup>To whom correspondence should be addressed. [rdkamm@mit.edu](mailto:rdkamm@mit.edu).<sup>†</sup>Equal contributions<sup>†</sup>Electronic Supplementary Information (ESI) available: Phase contrast images of cells in thermoplastic devices, details of device fabrication and cell culture, mathematical derivations.

A recent study presented an oxygen-impermeable cell culture device made from PMMA, equipped with oxygen sensors at the media inlet and outlet.<sup>17</sup> However, the locations of oxygen sensing does not allow for continuous analysis across the entire cell culture area. Other reports focus on the investigation of oxygen levels in gas-permeable PDMS devices during cell culture.<sup>18-24</sup> A range of commercial sensors has been developed to measure the oxygen levels in biological systems. These are mostly based on ratiometric imaging of fluorescence intensity or lifetime of oxygen-sensitive dyes embedded in sol-gel coatings (Ocean Optics, FL, USA) or polymer matrices (Visisens, Regensburg, Germany). In this communication, we experimentally determine and numerically simulate the oxygen levels prevailing in microfluidic devices under cell culture conditions. The proposed computational model represents a powerful tool to predict oxygen levels in microfluidic devices of known oxygen permeability and for different cell types with known oxygen uptake behaviour.

We used a simple, yet versatile chip design (Fig. 1A) with a central gel channel (to study cells in 3D biological matrices), and flanked by two media channels (for 2D cellular studies).<sup>25</sup> A thin layer (10  $\mu\text{m}$ ) of PDMS was spin-coated onto a commercial oxygen sensor foil, since direct bonding of foils and devices failed to produce stable bonds. PDMS is known to bond well to both PDMS and COC and has been used as a glue interlayer in similar systems.<sup>8, 9, 22, 26, 27</sup> The PDMS-coated foils were then irreversibly plasma-bonded to aminopropyltriethoxysilane (APTES)-modified thermoplastic chips or PDMS devices (Fig. 1B). PDMS coating, plasma treatments and thermal curing (80°C for >2 h) did not have a significant effect on sensor performance when compared to pristine foils.

We examined the oxygen consumption of two different cell types which are of interest for microfluidic cell culture applications: endothelial cells (EC) are frequently used for studies of angiogenesis and cancer metastasis,<sup>13</sup> whereas highly active hepatocytes (HEP) are of interest for liver tissue engineering and organ-on-a-chip applications.<sup>24, 28, 29</sup> Both cell types were independently seeded in the media channels of the microfluidic devices, cultured for the indicated time periods, and oxygen consumption was monitored. The oxygen levels at the start of the experiment (15-17%), differ from typical levels (21%), but accurately represent ambient pressure oxygen levels in cell culture media at 37 °C.<sup>30-32</sup>

HEP depleted almost all oxygen in the impermeable COC device, reaching 4% within 60 min (Fig. 2B), in agreement with previous studies.<sup>28, 29</sup> The mildly hypoxic conditions observed in PMP devices (<11%) are very similar to oxygen levels prevailing *in vivo*.<sup>13, 16</sup> In thin PDMS devices, however, oxygen is readily replenished from the environment, resulting in stabilization of oxygen levels at ~16% for both HEP and EC culture (Fig 2 A +B). The total PDMS thickness is known to have a significant influence on the oxygen levels,<sup>33</sup> and indeed HEP culture in 5 mm thick devices resulted in oxygen levels equilibrating around 11.5% (data not shown). Cell culture in PMP devices gave rise to intermediate oxygen levels in all cases due to its intrinsic properties (high oxygen permeability compared to COC), making PMP a promising candidate for commercial production of microfluidic cell culture devices.

Parallel to experimental evaluation, the oxygen consumption of HEP and ECs was numerically simulated for PDMS, PMP and COC devices as a function of oxygen uptake

rate (OUR, in units of  $\text{pmol s}^{-1}$  per  $10^6$  cells). For higher accuracy of the simulation, the actual cell numbers in the devices were assessed based on phase contrast images (Fig. S1). According to the intrinsic permeability of the material, a continuous partial pressure model was adopted for PDMS and PMP,<sup>24</sup> and a simple concentration-based model was solved in the fluid domain for the impermeable COC. In agreement with our experimental results, we observed that in thin, permeable PDMS devices the oxygen partial pressure remained at ambient levels ( $\sim 16\%$ , Fig. 2C & D) for both cell types. The minor differences ( $\sim 1\%$ ) between experimental and simulation data are attributed to errors in instrument calibration. For PMP devices, the oxygen consumption of EC was predicted accurately. The simulation for HEP in PMP was initially more conservative than observed experimentally. We attribute this to differences in the maximum OUR, which varies in literature between 380 and 700  $\text{pmol s}^{-1}$  per  $10^6$  cells.<sup>24, 28, 29</sup> Furthermore, PMP is still a new material, and its permeation properties may be sensitive to polymer processing history and film preparation methods, contributing to deviations between model and experiment.<sup>34</sup> For COC devices, oxygen levels stabilized at a moderate fixed OUR = 20 for EC culture (Fig. 2G), which compares well to literature values for human umbilical vein ECs (OUR = 19.9).<sup>13</sup> For HEP in COC and PMP, the experimental data followed an asymptotic behaviour, which could not be reproduced using a fixed OUR=500 in the simulations (Fig. 2H). These variations in respiratory activity over time are commonly attributed to “hepatic hibernation”, a feedback mechanism that allows the hepatocytes to maintain viability by decreasing their oxygen consumption in a hypoxic environment.<sup>13, 35-37</sup> In order to account for this dynamic behaviour, we implemented a variable function for the simulation of oxygen concentrations in COC devices (compare ESI). When a linear relationship between OUR and oxygen partial pressure was assumed, good match was achieved between experimental and simulation data (initial OUR=700 at 100 Torr  $\text{O}_2$ , decreasing to OUR=83 at 20 Torr  $\text{O}_2$ ).<sup>36</sup>

A simple way to counteract oxygen depletion in thermoplastic devices is to introduce media at a flow rate sufficient to balance the respective oxygen consumption rates. We remark that the culture of a dense layer of HEP in both media channels of the device is an extreme case of oxygen consumption. A simple mathematical model (compare ESI) was developed to calculate the minimum flow rates:  $0.0273 \mu\text{l s}^{-1}$  ( $2.36 \text{ mL day}^{-1}$ ) for HEP culture and  $0.0033 \mu\text{l s}^{-1}$  ( $0.29 \text{ mL day}^{-1}$ ) for ECs.<sup>23</sup> At flow rates of this magnitude, shear stresses fall in the range of 1.57 to 0.19 Pa, values at which the effect of shear forces on cell attachment or activation is negligible, except perhaps at the highest levels of shear stress.<sup>38, 39</sup> An alternative way to reoxygenate the cells in the device is to employ a thin oxygen-permeable film to close the channels on the bottom surface of the device (PDMS or PMP). Our calculations show that lamination with oxygen-permeable films is also capable of maintaining normoxic conditions during culture for laminate thicknesses of  $\sim 100 \mu\text{m}$  (see ESI).

In summary, we developed a computational model capable of estimating the cellular respiratory activity in microfluidic devices. *Vice versa*, the model can be used to predict oxygen levels in microfluidic devices for cell types with a known OUR. This provides a powerful and indispensable tool for research-based and industrial applications targeting oxygen-related cellular behaviour. We introduced PMP as a promising material for

industrial microfluidic application: PMP combines good oxygen permeability with excellent processability, and provides sufficient oxygen levels even for highly active cell types. Lastly, we demonstrated that moderate media flow rates or device lamination with oxygen-permeable films may be applied to counteract oxygen depletion in non-permeable thermoplastic devices.

## Materials and Methods

Details of device fabrication and cell culture can be found in the Electronic Supporting Information (S1 and S2). The Visisens handheld microscope was mounted vertically in a variable incubator and the microfluidic devices (bonded to sensor foils and filled with collagen gel and cells) were placed on top. The oxygen partial pressure in the device was monitored in the central 5 by 2.5 mm<sup>2</sup> area including the gel and adjoining media channels. All oxygen measurements were evaluated using the Visisens software (AnalytiCal 1, VA 1.11 prototype version) after calibration against two reference solutions. Oxygen-free solution was prepared by dissolving 1 g of sodium sulfite in 100 ml water with 50 ul of Co(NO<sub>3</sub>)<sub>2</sub> standard solution (1g l<sup>-1</sup> in 0.5 M nitric acid). Water bubbled with air for 30 min was used as a second calibration point (air-saturated). Due to the opaqueness of the oxygen-sensitive coating, control devices with a glass coverslip bottom were fabricated to facilitate visualization of cell morphology and distribution (Fig. S1). Excellent viability over 2 days of culture in all devices was observed, confirming earlier results with human endothelial cells.<sup>25</sup> Phase-contrast images were taken with a CCD color digital camera (Olympus DP72, Japan) connected to an inverted Olympus IX71 microscope. Images were captured with DP2 BSW Software (version 2.2) and analyzed by ImageJ software (Scion Corp., USA).

The oxygen consumption in the devices during EC or HEP culture was simulated using a commercial finite element software (COMSOL Multiphysics v4.2). Transport of diluted species equation (Fick's law) was adopted as the governing equation, considering the molar concentration of oxygen  $c$  as dependent variable. The computational mesh consisted of  $\sim 1.8 \times 10^6$  tetrahedral elements with a total volume of 410 mm<sup>3</sup>. To reduce the calculation time, only a quarter of the device was considered by imposing a symmetry condition on the two cutting planes. The cells were represented as a thin (10  $\mu$ m) layer on top of the PDMS glue layer. A no-flux condition was implemented to represent the impermeable oxygen sensor foil. A constant concentration of oxygen (17%) was considered as boundary condition on the surfaces exposed to the external environment (fluid channel and gel injection inlet). A time dependent simulation was solved for a period of 4 h at 10 min intervals. The diffusion coefficients and initial oxygen concentration in the different materials are summarized below.

## Supplementary Material

Refer to Web version on PubMed Central for supplementary material.

## Acknowledgments

This research was supported by the National Research Foundation Singapore through the Singapore MIT Alliance for Research and Technology's BioSystems and Micromechanics Inter-Disciplinary Research programme, and the

National Cancer Institute (1R33CA174550). We also acknowledge the Japan Society for Promotion of Science "Strategic Young Researcher Overseas Visits Program for Accelerating Brain Circulation," the Murata Overseas Scholarship Foundation and Mochida Memorial Foundation for Medical and Pharmaceutical Research.

## References

1. Duffy DC, McDonald JC, Schueller OJA, Whitesides GM. *Anal. Chem.* 1998; 70:4974–4984. [PubMed: 21644679]
2. Toepke MW, Beebe DJ. *Lab Chip.* 2006; 6:1484–1486. [PubMed: 17203151]
3. Opegard SC, Nam KH, Carr JR, Skaalure SC, Eddington DT. *PLoS One.* 2009; 4
4. Funamoto K, Zervantonakis IK, Liu YC, Ochs CJ, Kim C, Kamm RD. *Lab Chip.* 2012; 12:4855–4863. [PubMed: 23023115]
5. Lo JF, Sinkala E, Eddington DT. *Lab Chip.* 2010; 10:2394–2401. [PubMed: 20559583]
6. Allen CB, Schneider BK, White CW. *American Journal of Physiology-Lung Cellular and Molecular Physiology.* 2001; 281:L1021–L1027. [PubMed: 11557606]
7. Slepicka P, Trostova S, Kasalkova NS, Kolska Z, Malinsky P, Mackova A, Bacakova L, Svorcik V. *Polym. Degrad. Stabil.* 2012; 97:1075–1082.
8. Quaglio M, Canavese G, Giuri E, Marasso SL, Perrone D, Cocuzza M, Pirri CF. *J. Micromech. Microeng.* 2008; 18
9. Sunkara V, Park DK, Hwang H, Chantiwas R, Soper SA, Cho YK. *Lab Chip.* 2011; 11:962–965. [PubMed: 21152492]
10. Lee KS, Ram RJ. *Lab Chip.* 2009; 9:1618–1624. [PubMed: 19458871]
11. Kim K, Park SW, Yang SS. *BioChip J.* 2010; 4:148–154.
12. Ma KS, Reza F, Saaem I, Tian JD. *J. Mater. Chem.* 2009; 19:7914–7920.
13. Abaci HE, Truitt R, Luong E, Drazer G, Gerecht S. *Am. J. Physiol.-Cell Physiol.* 2010; 298:C1527–C1537. [PubMed: 20181925]
14. Guppy M, Brunner S, Buchanan M. *Comp. Biochem. Physiol. B-Biochem. Mol. Biol.* 2005; 140:233–239. [PubMed: 15649770]
15. Baze MM, Schlauch K, Hayes JP. *Physiol. Genomics.* 2010; 41:275–288. [PubMed: 20103700]
16. Tiede LM, Cook EA, Morsey B, Fox HS. *Cell Death & Disease.* 2011; 2:e246. [PubMed: 22190005]
17. Abaci HE, Devendra R, Smith Q, Gerecht S, Drazer G. *Biomed. Microdevices.* 2012; 14:145–152. [PubMed: 21947550]
18. Sud D, Mehta G, Mehta K, Linderman J, Takayama S, Mycek MA. *J. Biomed. Opt.* 2006; 11
19. Wang L, Liu WM, Wang YL, Wang JC, Tu Q, Liu R, Wang JY. *Lab Chip.* 2013; 13:695–705. [PubMed: 23254684]
20. Saito T, Wu CC, Shiku H, Yasukawa T, Yokoo M, Ito-Sasaki T, Abe H, Hoshi H, Matsue T. *Analyst.* 2006; 131:1006–1011. [PubMed: 17047800]
21. Vollmer AP, Probststein RF, Gilbert R, Thorsen T. *Lab Chip.* 2005; 5:1059–1066. [PubMed: 16175261]
22. Wang L, Acosta MA, Leach JB, Carrier RL. *Lab Chip.* 2013; 13:1586–1592. [PubMed: 23443975]
23. Mehta G, Mehta K, Sud D, Song JW, Bersano-Begey T, Futai N, Heo YS, Mycek MA, Linderman JJ, Takayama S. *Biomed. Microdevices.* 2007; 9:123–134. [PubMed: 17160707]
24. Kim MC, Lam RHW, Thorsen T, Asada HH. *Microfluidics and Nanofluidics.* 2013; 15:285–296.
25. Jeon JS, Chung S, Kamm RD, Charest JL. *Biomed. Microdevices.* 2011; 13:325–333. [PubMed: 21113663]
26. Mehta G, Lee J, Cha W, Tung YC, Linderman JJ, Takayama S. *Anal. Chem.* 2009; 81:3714–3722. [PubMed: 19382754]
27. Xu BY, Yan XN, Xu JJ, Chen HY. *Biomicrofluidics.* 2012; 6
28. Cho CH, Park J, Nagrath D, Tilles AW, Berthiaume F, Toner M, Yarmush ML. *Biotechnol. Bioeng.* 2007; 97:188–199. [PubMed: 17054120]

29. Nahmias Y, Kramvis Y, Barbe L, Casali M, Berthiaume F, Yarmush ML. *Faseb J.* 2006; 20:E1828–E1836.
30. Lee S, They BL, Cote GL, Pishko MV. *Sensors and Actuators B-Chemical.* 2008; 128:388–398.
31. Naciri M, Kuystermans D, Al-Rubeai M. *Cytotechnology.* 2008; 57:245–250. [PubMed: 19003181]
32. Newby D, Marks L, Lyall F. *Placenta.* 2005; 26:353–357. [PubMed: 15823622]
33. Cox ME, Dunn B. *J. Polym. Sci. Pol. Chem.* 1986; 24:621–636.
34. Merkel TC, Freeman BD, Spontak RJ, He Z, Pinnau I, Meakin P, Hill AJ. *Chem. Mat.* 2003; 15:109–123.
35. Chandel NS, Budinger GRS, Choe SH, Schumacker PT. *Journal of Biological Chemistry.* 1997; 272:18808–18816. [PubMed: 9228055]
36. Subramanian RM, Chandel N, Budinger GRS, Schumacker PT. *Hepatology.* 2007; 45:455–464. [PubMed: 17366663]
37. Clementi E, Brown GC, Foxwell N, Moncada S. *Proc. Natl. Acad. Sci. U. S. A.* 1999; 96:1559–1562. [PubMed: 9990063]
38. Lu H, Koo LY, Wang WCM, Lauffenburger DA, Griffith LG, Jensen KF. *Anal. Chem.* 2004; 76:5257–5264. [PubMed: 15362881]
39. Tilles AW, Baskaran H, Roy P, Yarmush ML, Toner M. *Biotechnol. Bioeng.* 2001; 73:379–389. [PubMed: 11320508]

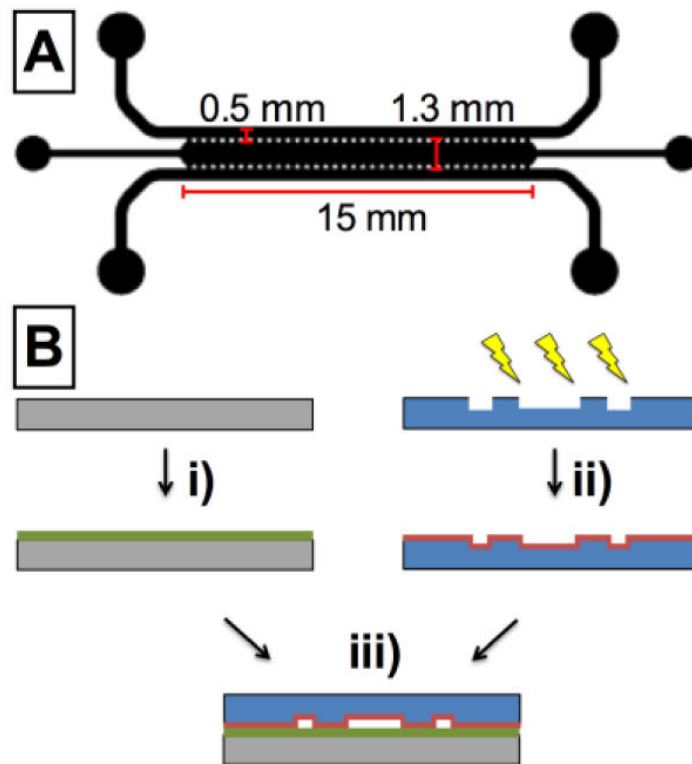


**Figure 1.** (A) Schematic of the microfluidic chip design and dimensions. Channel height is 150  $\mu\text{m}$ , post width and spacing is 125  $\mu\text{m}$ . (B) Device assembly: i) oxygen sensor foil is spin-coated with PDMS. ii) plasma-activated thermoplastic is exposed to APTES solution. iii) plasma-bonding of substrate and chip.

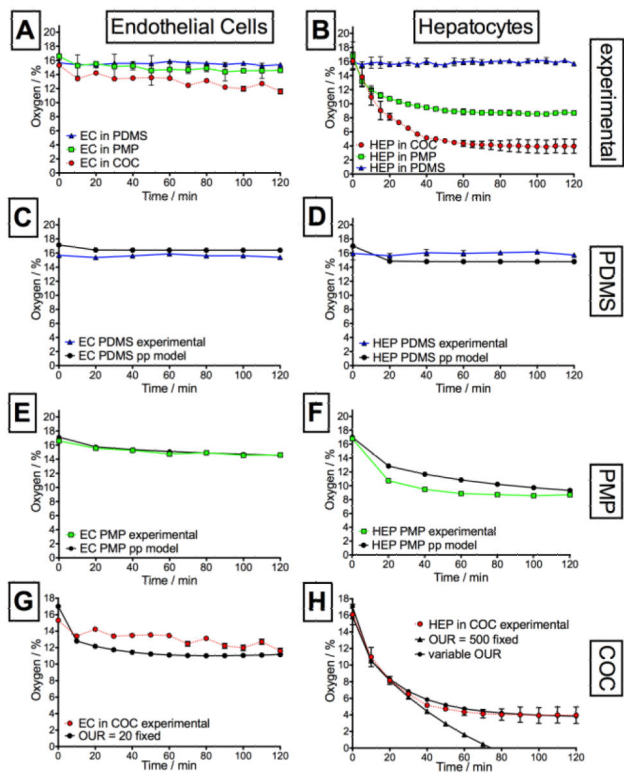


**Figure 2.** Summary of experimental (A+B) and simulated oxygen levels (C-H) for endothelial and hepatocytes culture in microfluidic devices made from PDMS (C+D), PMP (E+F) and COC (G+H). Coloured symbols represent experimental data, which are compared to simulation results (black symbols).



**Table 1**

Physical properties used in the simulations

Material	$D_{O_2}$ ( $m^2 s^{-1}$ )	Initial $O_2$ (%)
Media, gel, cells	$3.35 \times 10^{-9}$	17
PDMS	$4.0 \times 10^{-9}$	17
PMP	$2.315 \times 10^{-11}$	17
COC	0	0